

NWPU-Crowd: A Large-Scale Benchmark for Crowd Counting

Qi Wang, *Senior Member, IEEE*, Junyu Gao, *Student Member, IEEE*, Wei Lin, Xuelong Li*, *Fellow, IEEE*

Abstract—In the last decade, crowd counting attracts much attention of researchers due to its wide-spread applications, including crowd monitoring, public safety, space design, etc. Many Convolutional Neural Networks (CNN) are designed for tackling this task. However, currently released datasets are so small-scale that they can not meet the needs of the supervised CNN-based algorithms. To remedy this problem, we construct a large-scale congested crowd counting dataset, NWPU-Crowd, consisting of 5, 109 images, in a total of 2, 133, 238 annotated heads. Compared with other real-world datasets, it contains various illumination scenes and has the largest density range ($0 \sim 20, 033$). Besides, a benchmark website is developed for impartially evaluating the different methods, which allows researchers to submit the results of the test set. Based on the proposed dataset, we further describe the data characteristics, evaluate the performance of some mainstream state-of-the-art (SOTA) methods, and analyze the new problems that arise on the new data. What's more, NWPU-Crowd Dataset is available at <http://www.crowdbenchmark.com/>, and the code is open-sourced at <https://github.com/gjy3035/NWPU-Crowd-Sample-Code>.

Index Terms—Crowd counting, crowd analysis, benchmark website, density map regression.

1 INTRODUCTION

CROWD analysis is an essential task in the field of video surveillance. Accurate analysis for crowd motion, human behavior, population density is crucial to public safety, urban space design, etc. Crowd counting, a subtask of crowd analysis, provides the pixel-wise density distribution and scene-level counting number, which is the basic information for pedestrians and the core of crowd scenes. Due to the importance of crowd counting, many researchers [1], [2], [3], [4], [5] pay attention to it and achieve quite a few significant improvements in this field. Especially, benefiting from the development of deep learning in computer vision, the counting performance on the datasets [6], [7], [8], [9] is continuously refreshed by Convolutional Neural Networks (CNN)-based methods [10], [11], [12], [13], [14].

The CNN-based methods need to learn discriminate features from a multitude of labeled data, so a large-scale dataset can effectively promote the development of visual technologies. It is verified in many existing tasks, such as object detection [15], [16] and semantic segmentation [17], [18]. However, the currently released crowd counting datasets are so small-scale that most deep-learning-based methods are prone to overfit the data. According to the statistics, UCF-QNRF [9] is the largest released congested crowd counting dataset. Still, it contains only 1, 535 samples, in a total of 1.25 million annotated instances, which is still unable to meet the needs of current deep learning methods. Moreover, there is not an impartial evaluation benchmark, which potentially restricts further development of crowd counting. By

the way, some methods¹ may use mistaken labels to evaluate models, which is also not accurate. Reviewing some benchmarks in other fields, KITTI [19], CityScapes [20], and Microsoft COCO [16], they allow the researchers to submit their results of the test set and impartially evaluate them, which facilitates the study of methodology. Thus, an equitable evaluation platform is important for the community.

Considering the problems mentioned above, in this paper, we construct a large-scale crowd counting dataset, named as **NWPU-Crowd**, and develop a benchmark website to boost the community of crowd counting. Compared with the existing congested datasets, the proposed NWPU-Crowd has the following main advantages: 1) This is the largest crowd counting dataset, consisting of 5, 109 images and containing 2, 133, 238 annotated instances; 2) It introduces some negative samples like high-density crowd images to assess the robustness of models; 3) In NWPU-Crowd, the number of annotated objects range, $0 \sim 20, 033$. More concrete features are described in Section 3.3. Table 1 illustrates the detailed statistics of nine mainstream real-world datasets and the proposed NWPU-Crowd. Since JHU-dataset is not released, we use a gray background for it in the table.

Based on the proposed NWPU-Crowd, several experiments of some classical and state-of-the-art methods are conducted. After further analyzing their results, an interesting phenomenon on the proposed dataset is found: diverse data makes it difficult for counting networks to learn useful and distinguishable features, which does not appear or is ignored in the previous datasets. Specifically, 1) there are many error estimations on negative samples; 2) the data of different scene attributes (density level and luminance) have a significant influence on each other. Therefore, it is a research trend on how to alleviate the above two problems.

In summary, we believe that the proposed large-scale dataset will promote the application of crowd counting in practice and

• Qi Wang, Junyu Gao, Wei Lin, and Xuelong Li are with the School of Computer Science and with the Center for Optical Imagery Analysis and Learning (OPTIMAL), Northwestern Polytechnical University, Xi'an 710072, Shaanxi, China. E-mails: crabwq@gmail.com, gjy3035@gmail.com, elonlin24@gmail.com, xuelong_li@nwpu.edu.cn.

* Corresponding author: Xuelong Li.

1. <https://github.com/gjy3035/Awesome-Crowd-Counting/issues/78>

TABLE 1

Statistics of the nine mainstream real-world datasets and NWPU-Crowd (JHU-CORWD is unreleased, so we use the gray background for it).

Dataset	Number of Images	Avg. Resolution ($H \times W$)	Count Statistics				Extreme Congestion	Unseen Test Labels	Category-wise Evaluation
			Total	Min	Ave	Max			
UCSD [6]	2,000	158×238	49,885	11	25	46	✗	✗	✗
Mall [21]	2,000	480×640	62,325	13	31	53	✗	✗	✗
WorldExpo'10 [8]	3,980	576×720	199,923	1	50	253	✗	✗	✓
ShanghaiTech Part B [7]	716	768×1024	88,488	9	123	578	✗	✗	✗
Crowd_Surv [22]	13,945	840×1342	386,513	2	35	1,420	✗	✗	✗
UCF_CC_50 [23]	50	2101×2888	63,974	94	1,279	4,543	✓	✗	✗
ShanghaiTech Part A [7]	482	589×868	241,677	33	501	3,139	✓	✗	✗
UCF-QNRF [9]	1,535	2013×2902	1,251,642	49	815	12,865	✓	✗	✗
JHU-CROWD [24]	4,250	1450×900	1,114,785	-	262	7,286	✓	-	✓
NWPU-Crowd	5,109	2311×3383	2,133,238	0	418	20,033	✓	✓	✓

attract more attention to tackling the aforementioned problems.

2 RELATED WORKS

The existing crowd counting datasets mainly contain two types: surveillance-scene datasets and free-view datasets. The former commonly records crowd in particular scenarios, of which the data consistency is obvious. For the latter, the crowd samples are collected from the Internet. Thus, there are more perspective variations, occlusions, and extreme congestion in these datasets. Tabel 1 demonstrates a summary of the basic information of the mainstream crowd counting datasets, and in the following parts, their unique characters are briefly introduced.

2.1 Surveillance-scene Dataset

Surveillance view. Surveillance-view datasets aim to collect the crowd images in specific indoor scenes or small-area outdoor locations, such as marketplace, walking street, and station. The number of people usually ranges from 0 to 600. UCSD is a typical dataset for crowd analysis. It contains 2,000 image sequences, which records a pedestrian walk-way at the University of California at San Diego (UCSD). Mall [21] is captured in a shopping mall with more perspective distortion. However, these two datasets contain only a single scene, lacking data diversity. Thus, Zhang *et al.* [8] build a multi-scene crowd counting dataset, WorldExpo'10, consisting of 108 surveillance cameras with different locations in Shanghai 2010 WorldExpo, e.g., entrance, ticket office. Considering the poor resolution of traditional surveillance cameras, Zhang *et al.* [7] construct a high-quality crowd dataset, ShanghaiTech Part B, containing 782 images captured in some famous resorts of Shanghai, China. To remedy the occlusion problem in congested scenes, a multi-view dataset is designed by Zhang and Chan [25]. By equipping 5 cameras at different positions for a specific view, the data can be recorded synchronously. For getting rid of the manually labeling process, Wang *et al.* [26] construct a large-scale synthetic dataset. By simulating the perspective of a surveillance camera, they capture 400 crowd scenes in a computer game (Grand Theft Auto V, GTA V), a total of 15,212 images.

In addition to the aforementioned datasets, there are also other crowd counting datasets with their specific characteristics. SmartCity [27] and Beijing-BRT [28] respectively focus on some typical scenes, such as sidewalk and subway. ShanghaiTechRGBD [29] records the RGBD crowd images with a stereo camera for concentrating on pedestrian counts and localization.

Fudan-ShanghaiTech [30] and Venice [31] capture the video sequences for temporal crowd counting.

Drone view. For some big scenes (such as stadium, plaza) or some large rally events (ceremony, hajj, *etc.*), the above traditional fixed surveillance camera is not suitable due to its small field of view. To tackle this problem, some other datasets are collected through the Drone or Unmanned Aerial Vehicle (UAV). Benefiting from their higher altitudes, more flexible view and free flight, more large scenes can be recorded compared with the traditional surveillance camera. There are two crowd counting datasets with the drone view, DLR-ACD Dataset [32] and DroneCrowd Dataset [33]. The former consists of 33 images with 226,291 annotated persons, including some mass events: sports, concerts, trade fair, *etc.* The latter consists of 70 crowd scenes (such as campus, playground, and plaza), with a total of 33,600 drone-view image sequences. Due to the Bird's-Eye View (BEV), the whole body of pedestrians can not be seen except their heads, so the perspective change rarely appears in the above two datasets.

2.2 Free-view Dataset

In addition to the above crowd images captured in specific scenes, there are also many free-view crowd counting datasets, which are collected from the Internet. A remarkable aspect of free-view is that the crowd density varies significantly, which ranges from 0 to 20,000. Besides, diversified scenarios, light and shadow conditions, and uneven crowd distribution in one single image are also distinctive attributes of these datasets.

The first free-view dataset for crowd counting, UCF_CC_50 [23], is presented by Idrees *et al.* in 2013. It only contains 50 images, which is so small to train a robust deep learning model. Consequently, a larger crowd counting dataset becomes more significant nowadays. Zhang *et al.* propose ShanghaiTech Part A [7], which is constructed of 482 images crawled from the Internet. Although its average number of labeled heads in each image is smaller than UCV_CC_50, it contains more pictures and larger number of labeled head points. For further research on the extremely congested crowd counting, UCF-QNRF [9] is presented by Idrees *et al.* It is composed of 1,525 images with more than 1,251,642 label points. The average number of pedestrians per image is 815, and the maximum number reaches 12,865. Aiming at the small size of crowd images, Crowd Surveillance [22] build a large-scale dataset containing 13,945 images, which provides regions of interest (ROI) for each image to keep out these blobs that are ambiguous for training or testing. In addition to the above

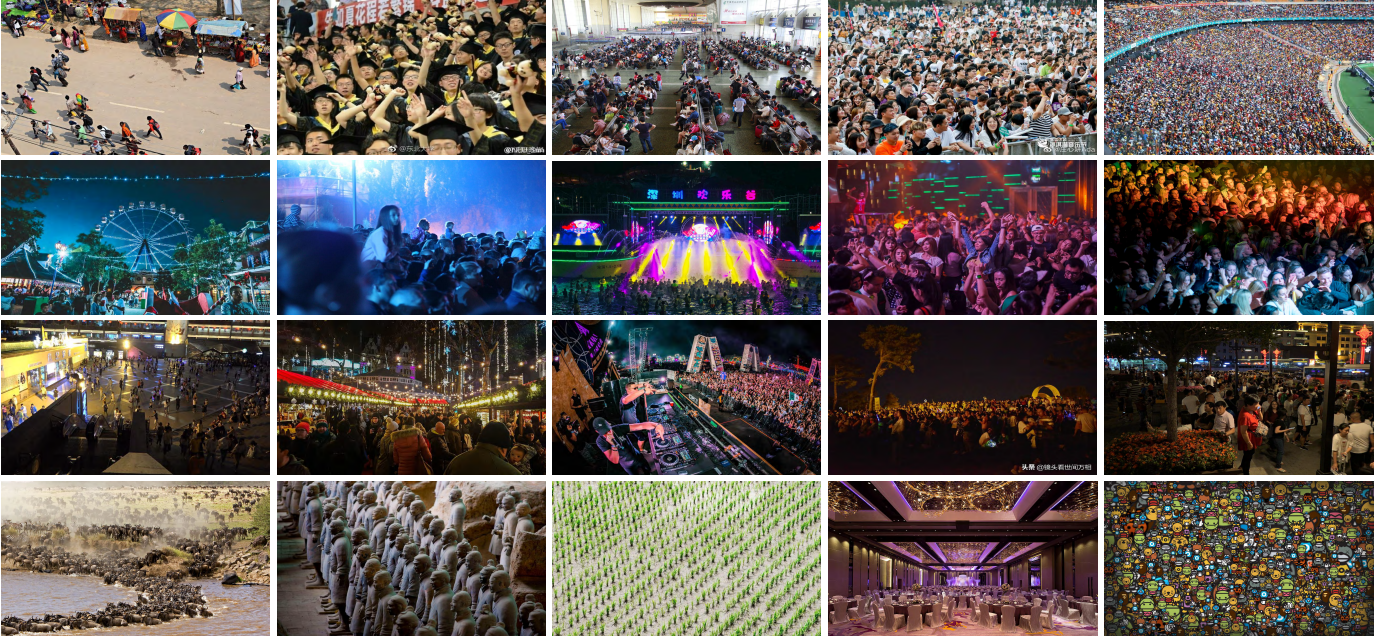


Fig. 1. The display of the proposed NWPU-Crowd dataset. Column 1 shows some typical samples with normal lighting. The second and third column demonstrate the crowd scenes under the extreme brightness and low-luminance conditions, respectively. The last column illustrates the negative samples, including some scenes with densely arranged other objects.

datasets, Sindagi *et al.* introduce a new dataset for unconstrained crowd counting, JHU-CROWD, including 4,250 samples. All images are annotated from the image and head level. For the former level, they label the scenario (*mall*, *stadium*, etc.) and weather conditions. For the head level, the annotation information includes not only head locations but also occlusion, size, and blur attributes.

3 NWPU-CROWD DATASET

This section describes the proposed NWPU-Crowd from four perspectives: data collection/specification, annotation tool, statistical analysis, data split and evaluation protocol.

3.1 Data Collection and Specification

Data Source. Our data are collected from self-shooting and the Internet. For the former, $\sim 2,000$ images and ~ 200 video sequences are captured in some populous Chinese cities, including Beijing, Shanghai, Chongqing, Xi'an, and Zhengzhou, containing some typical crowd scenes, such as resort, walking street, campus, mall, plaza, museum, station. However, extremely congested crowd scenes are not the norm in real life, which is hard to capture via self-shooting. Therefore, we also collect $\sim 8,000$ samples from some image search engines (Google, Baidu, Bing, Sougou, etc.) via the typical query keywords related to the crowd. Table 2 lists the primary data source websites and the corresponding keywords. The third row in the table records some Chinese websites and keywords. Finally, by the above two methods, 10,257 raw images are obtained.

Data Deduplication and Cleaning. We employ four individuals to download data from the Internet on non-overlapping websites. Even so, there are still some images that contain the same content. Besides, some congested datasets (UCF_CC_50, Shanghai Tech Part A, and UCF-QNRF), are also crawled from the Internet, e.g., Flickr, Google, etc. For avoiding the problem of data duplication,

TABLE 2
The query keywords on some mainstream search engine sites.

Data Source	Keywords
google, baidu, bing, pxhere, pixabay...	crowd, congestion, hundreds/thousands of people, speech, conference, ceremony, stadium, gathering, parade, demonstration, protest, hajj, carnival, beer festival, F1, NBA, WorldCup, NFL, EPL, Super Bowl, etc.
baidu, weibo, sogou, so, wallhere...	人群, 拥挤, 春运, 军训, 典礼, 祭祀, 庙会, 游客, 万人, 千人, 大赛, 运动会, 候车厅, 音乐会/节, 见面会, 人从众, 黄金周, 招聘会, 万人空巷, 人山人海, 摩肩接踵, 水泄不通.....

we perform an effective strategy, which is inspired by Perceptual Loss [34]. Specifically, for each image, the layer-wise VGG-16 [35] features (from conv1 to conv5_3 layer) are extracted. Then remove excess similar images by computing the distance of the feature between any two samples. Furthermore, some blurred images that are difficult to recognize the head location are also removed. Consequently, we obtain 5,109 valid images.

3.2 Data Annotation

Annotation tools: For conveniently annotating head points in the crowd images, an online efficient annotation tool is developed based on HTML5 + Javascript + Python. This tool supports two types of label form, namely point and bounding box. During the annotation process, each image is flexibly zoomed in/out to annotate head with different scales, and it is divided into 16×16 small blocks at most, which allows annotators to label the head under five scales: 2^i ($i=0,1,2,3,4$) times size of the original image. It effectively prompts annotation speed and quality. The more detailed description is shown in the video demo at <https://www.youtube.com/watch?v=U4Vc6bOPxm0>.

Annotation process: The entire annotation process has two stages: labeling and refinement. Firstly, there are 30 annotators involved in the initial labeling process, which costs 2,100 hours totally to annotate all collected images. After this, 6 individuals

are employed to refine the preliminary annotations, which takes 150 hours per refiner. In total, the entire annotation process costs 3,000 human hours.

3.3 Data Characteristic

NWPU-Crowd dataset consists of 5,109 images, with 2,133,238 annotated instances. Compared with the existing crowd counting datasets, it is the largest from the perspective of image and instance level. Fig. 1 respectively demonstrates four groups of typical samples from Row 1 to 4 in the dataset: normal-light, extreme-light, dark-light, and negative samples. Fig. 2 compares the number distribution of different counting range on three datasets: NWPU-Crowd, UCF-QNRF [9] and ShanghaiTech Part A [7]. In each bin, the number of images on NWPU-Crowd is much larger than that on the other two datasets. In addition to data volume, NWPU-Crowd has four more advantages compared with the previous datasets:

- 1) **Negative Samples.** NWPU-Crowd introduces 351 negative samples (namely nobody scenes), which are similar to congested crowd scenes in terms of texture features. It effectively improves the generalization of counting models while applied in the real world. These samples contain animal migration, fake crowd scenes (sculpture, Terra-Cotta Warriors, 2-D cartoon figure, etc.), empty hall, and other scenes with densely arranged objects that are not the person.
- 2) **Fair Evaluation.** For a fair evaluation, the labels of the test set are not public. Therefore, we develop an online evaluation benchmark website that allows researchers to submit their estimation results of the test set. The benchmark can calculate the error between presented results and ground truth, and list them on a scoreboard.
- 3) **Higher Resolution.** The proposed dataset collects high-quality and high-resolution scenes, which is entailed for extremely congested crowd counting. From Table 1, the average resolution of NWPU-Crowd is 2311×3383 , which is larger than that of other datasets. Specifically, the maximum image size is 4028×19044 .
- 4) **Large Appearance Variation.** NWPU-Crowd is a large-range-number counting dataset, of which the number of people ranges from 0 to 20,033. It causes large appearance variations within the data, since the visual patterns of sparse crowds are very different from that of the congested scenes, and the head scales in the two types of conditions are also different.

In summary, NWPU-Crowd is one of the largest and most challenging crowd counting datasets at present.

3.4 Data Split and Evaluation Protocol

NWPU-Crowd Dataset is randomly split into three parts, namely *training*, *validation* and *test* sets, which respectively contain 3,109, 500 and 1,500 images. Following some previous works, we adopt three metrics to evaluate the counting performance, which are Mean Absolute Error (MAE), Mean Squared Error (MSE), and mean Normalized Absolute Error (NAE). They can be formulated as follows:

$$MAE = \frac{1}{N} \sum_{i=1}^N |y_i - \hat{y}_i|, \quad (1)$$

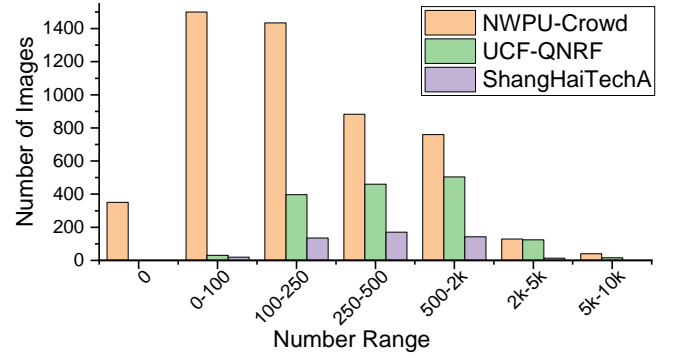


Fig. 2. The statistical histogram of crowd counts on the proposed NWPU-Crowd and other two mainstream congested datasets.

$$MSE = \sqrt{\frac{1}{N} \sum_{i=1}^N |y_i - \hat{y}_i|^2}, \quad (2)$$

$$NAE = \frac{1}{N} \sum_{i=1}^N \frac{|y_i - \hat{y}_i|}{y_i}, \quad (3)$$

where N is the number of images, y_i is the counting label of people and \hat{y}_i is the estimated value for the i -th test image. Since NWPU-Crowd contains quite a few negative samples, NAE's calculation does not contain them to avoid zero denominators.

In addition to the aforementioned overall evaluation on *the test set*, we further assess the model from different perspectives: scene level and luminance. The former have five classes according to the number of people: 0, (0, 100], (100, 500], (500, 5000], and more than 5000. The latter have three classes based on luminance value in the YUV color space: [0, 0.25], (0.25, 0.5], and (0.5, 0.75]. The two attribute labels are assigned to each image according to their annotated counting number and image contents. For each class in a specific perspective, MAE, MSE, and NAE are applied to the corresponding samples in *the test set*. Take the luminance attribute as an example, the average values of MAE, MSE, and NAE at the three categories can reflect counting models' sensitivity to the luminance variation. Similar to the overall metrics, the negative samples are excluded during the calculation of NAE.

4 EXPERIMENTS

In this section, we train nine mainstream open-sourced methods on the proposed NWPU-Crowd and submit their results on the evaluation benchmark. Besides, the further experimental analysis and visualization results on *the validation set* are discussed.

4.1 Participation Methods

MCNN [7]: Multi-Column Convolutional Neural Network. It is a classical and lightweight counting model, proposed by Zhang *et al.* in 2016. Different from the original MCNN, the RGB images are fed into the network.

SANet [36]: Scale Aggregation Network. SANet is an efficient encoder-decoder network with Instance Normalization for crowd counting, which combines the MSE loss and SSIM loss to output the high-quality density map.

PCC Net [37]: Perspective Crowd Counting Network. It is a multi-task network, which tackles the following tasks: density-level classification, head region segmentation, and density map



Fig. 3. The eight groups of visualization results of some selected methods on *the validation set*.

regression. The authors provide two versions, a lightweight from scratch and VGG-16 backbone.

C3F-VGG [38]: A simple baseline based on VGG-16 backbone for crowd counting. C3F-VGG consists of the first 10 layers of VGG-16 [35] as image feature extractor and two convolutional layers with a kernel size of 1 for regressing the density map.

CSRNet [12]: Congested Scene Recognition Network. CSRNet is a classical and efficient crowd counter, proposed by Li *et al.* in 2016. The authors design a Dilatation Module and add it to the top of the VGG-16 backbone. This network significantly improves performance in the field of crowd counting.

CANNet [39]: Context-Aware Network. CANNet combines the features of multiple streams using different respective field sizes. It encodes the multi-scale contextual information of the crowd scenes and yields a new record on the mainstream datasets.

SCAR [40]: Spatial-/Channel-wise Attention Regression Networks. SCAR utilizes the self-attention module [41] on the spatial and channel axis to encode the large-range contextual information. The well-designed attention models effectively extracts discrimi-

native features and alleviates mistaken estimations.

BL [42]: Bayesian Loss for Crowd Count Estimation. Different from the traditional strategy for the generation of ground truth, BL design a loss function to directly using head point supervision. It achieves state-of-the-art performance on the UCF-QNRF dataset.

SFCN[†] [26] Spatial Fully Convolutional Network with ResNet-101 [43]. SFCN[†] is the only crowd counting model that uses ResNet-101 as a backbone, which shows the powerful capacity of density regression on the congested crowd scenes.

4.2 Implementation Details

In the experiments, for PCC Net² and BL³, the models are trained using the official codes and the default parameters. For SANet, we implement the C³ Framework [38] and follow the corresponding parameters to train them on NWPU-Crowd dataset.

For other models, namely MCNN, CSRNet, C3F-VGG, CANNet, SCAR, and SFCN[†], they are reproduced in our counting

2. <https://github.com/gjy3035/PCC-Net>

3. <https://github.com/ZhihengCV/Bayesian-Crowd-Counting>

TABLE 3

The leaderboard of the counting performance on the NWPU-Crowd test set. In the ranking strategy, the Overall MAE is the primary key. “FS” represents that the model is trained From Scratch, without any pre-trained model. $S_0 \sim S_4$ respectively indicates five categories according to the different number range: 0, (0, 100], (100, 500], (500, 5000], and ≥ 5000 . $L_0 \sim L_2$ respectively denotes three luminance levels on *the test set*: [0, 0.25], (0.25, 0.5], and (0.5, 0.75]. Limited by the paper length, only MAE are reported in the category-wise results. The speed and FLOPs are computed on the input size of 576×768 . The red, blue and green color respectively represent the first, second and third place of the leaderboard.

Method	Backbone	Overall			Scene Level (only MAE)			Luminance (only MAE)		Model Size (M)	Speed (fps)	GFLOPs
		MAE	MSE	NAE	Avg.	$S_0 \sim S_4$		Avg.	$L_0 \sim L_2$			
MCNN	FS	232.5	714.6	1.063	1171.9	356.0/72.1/103.5/509.5/4818.2		220.9	472.9/230.1/181.6	0.133	129.0	11.867
SANet	FS	190.6	491.4	0.991	716.3	432.0/65.0/104.2/385.1/2595.4		153.8	254.2/192.3/169.7	1.389	10.8	40.195
PCC-Net-light	FS	167.4	566.2	0.444	944.9	85.3/25.6/80.4/424.2/4108.9		141.2	253.1/167.9/144.9	0.504	12.6	72.797
C3F-VGG	VGG-16	127.0	439.6	0.411	666.9	140.9/26.5/58.0/307.1/2801.8		127.9	296.1/125.3/91.3	7.701	47.2	123.524
CSRNet	VGG-16	121.3	387.8	0.604	522.7	176.0/35.8/59.8/285.8/2055.8		112.0	232.4/121.0/95.5	16.263	26.1	182.695
PCC-Net-VGG	VGG-16	112.3	457.0	0.251	777.6	103.9/13.7/42.0/259.5/3469.1		111.0	251.3/111.0/82.6	10.207	24.0	145.157
CANNet	VGG-16	106.3	386.5	0.295	612.2	82.6/14.7/46.6/269.7/2647.0		102.1	222.1/104.9/82.3	18.103	22.0	193.580
SCAR	VGG-16	110.0	495.3	0.288	718.3	122.9/16.7/46.0/241.7/3164.3		102.3	223.7/112.7/73.9	16.287	24.5	182.856
BL	VGG-19	105.4	454.2	0.203	750.5	66.5/8.7/41.2/249.9/3386.4		115.8	293.4/102.7/68.0	21.449	34.7	182.186
SFCN [†]	ResNet-101	105.7	424.1	0.254	712.7	54.2/14.8/44.4/249.6/3200.5		106.8	245.9/103.4/78.8	38.597	8.8	272.763

experiments, which is developed based on C^3 Framework [38], an open-sourced crowd counting project using PyTorch [44]. In the data pre-processing stage, the high-resolution images are resized to the 2048-px scale with the original aspect ratio. The density map is generated by a Gaussian kernel with a fixed size of 15 and the σ of 4. For augmenting the data, during the training process, all images are randomly cropped with the size of 576×768 , flipped horizontally, transformed to gray-scale images, and gamma corrected with a random value in [0.4, 2]. To optimize the above counting networks, Adam algorithm [45] is employed. Other parameters (such as learning rate, batch size) are reported in <https://github.com/gjy3035/NWPU-Crowd-Sample-Code>.

4.3 Results Analysis on the Validation Set

Quantitative Results. Here, we list the counting performance and density quality of all participation methods in Table 4. For evaluating the quality of the density map, two popular criteria are adopted, Peak Signal-to-Noise Ratio (PSNR) and Structural Similarity in Image (SSIM) [46]. Since BL [42] is supervised by point locations instead of density maps, PSNR and SSIM are not reported. In the calculation of PSNR, the negative samples are excluded to avoid zero denominators.

TABLE 4
The performance of different models on *the validation set*.

Method	<i>the validation set</i>			
	MAE	MSE	PSNR	SSIM
MCNN	218.53	700.61	28.558	0.875
SANet	171.16	471.51	29.228	0.886
PCC-Net-light	141.37	630.72	29.745	0.937
C3F-VGG	105.79	504.39	29.977	0.918
CSRNet	104.89	433.48	29.901	0.883
PCC-Net-VGG	100.77	573.19	30.565	0.941
CANNet	93.58	489.90	30.428	0.870
SCAR	81.57	397.92	30.356	0.920
BL	93.64	470.38	-	-
SFCN [†]	95.46	608.32	30.591	0.952

From the table, we find SCAR [40] attains the best counting performance, MAE of 81.57 and MSE of 397.92. SFCN[†] [26]

produces the most high-quality density maps, PSNR of 30.591 and SSIM of 0.952. For the three light models (MCNN, SANet, PCC-Net-light), we find that the last achieves the best SSIM (0.937), which even surpasses the SSIMs of some other VGG-based algorithms, such as C3F-VGG, CSRNet, CANNet, and SCAR. Similarly, PCC-Net-VGG is the best SSIM in the VGG-backbone methods.

Visualization Results. Fig. 3 demonstrates some predicted density maps of the eight methods. The first two columns are negative samples, and others are crowd scenes with different density levels. From the first two columns, almost all models perform poorly for negative samples, especially densely arranged objects. For humans, we can easily recognize that the two samples are mural and stones. But for the counting models, they cannot understand them. For the third column, although the predictions of these methods are good, there are still many mistaken errors in background regions. For the last two images that are extremely congested scenes, the estimation counts are far from the ground truth. SCAR is the most accurate method on *the validation set*, but it is about 1,900 and 8,000 people away from the labels, respectively. For the extreme-luminance scenes (Image 3367, 3250, and 3353), there are quite a few estimation errors in the high-light or dark-light regions. In general, the ability of the current models to cope with the above hard samples needs to be further improved.

4.4 Leaderboard

Table 3 reports the results of the participation methods on *the test set*. It lists the overall performance (MAE, MSE, and NAE), category-wise MAE on the attribute of scene level and luminance, model size, speed (inference time) and floating-point operations per second (FLOPs)⁴. Compared with the results of *the validation set*, we find that the ordering has changed significantly. Although SCAR attains the best results of MAE and MSE on *the validation set*, the performance on *the test set* is not good. For the primary key (overall MAE), BL, SFCN[†] and CANNet occupy the top three on *the test set*.

From the category-wise results of Scene Level, we find that all methods perform poorly in S_0 (negative samples), S_3 ((500, 5000]) and S_4 (≥ 5000), which causes that the average

4. For PCC-Net, we remove the useless layers (classification and segmentation modules) to compute the last three items: model size, speed and FLOPs.

value of category-wise MAE is larger than the overall MAE (SFCN†: 712.7 v.s. 105.7). Besides, this phenomenon shows that negative samples and congested scenes are more challenging than sparse crowd images. Similarly, for the luminance classes, the MAE of $L0$ ($[0, 0.25]$) is larger than that of $L1$ and $L2$. In other words, the counters work better under the standard luminance than under the low-luminance scenes.

Limited by the paper length, we only list some critical metrics in the table. More detailed results are shown in <https://www.crowdbenchmark.com/nwpucrowd.html>.

4.5 Discussion of Inter-category Impact

From Section 4.3 and 4.4, we find that two interesting phenomena worth attention: 1) Negative samples are prone to be mistakenly estimated; 2) The data with different scene attributes (namely density level) significantly affect each other. In this section, we conduct two experiments using a simple baseline model, C3F-VGG [38], to explore the above problems.

Phenomenon 1. For the first problem, the main reason is that the negative samples contain densely arranged objects, which is similar to the congested crowd scenes. As we all know, most existing counting models focus on texture information and local patterns for congested regions. To verify our thoughts, we design three groups of experiments to explore which samples affect the performance of negative samples. To be specific, we train three C3F-VGG counters on different combination training data: $S0 + S1$, $S0 + S2$, and $S0 + S3 + S4$ (considering that the number of $S4$ is small, so we integrate $S3$ and $S4$). Then the evaluation is performed on *the validation set*. Finally, the corresponding performance is listed in Table 5. From it, the MAE on Negative Sample ($S0$) increases from 18.54 to 147.53 as the density of positive samples increases.

TABLE 5
The MAE of the different data combination on *the validation set*.

Combination	<i>the validation set</i>				
	$S0$	$S1$	$S2$	$S3$	$S4$
$S0 + \dots + S4$	61.25	<u>28.53</u>	<u>51.91</u>	<u>188.66</u>	<u>3730.56</u>
$S1 + \dots + S4$	-	33.12	68.63	238.88	3997.57
$S0 + S1$	18.54	<u>16.44</u>	-	-	-
$S1$	-	21.00	-	-	-
$S0 + S2$	64.68	-	<u>49.97</u>	-	-
$S2$	-	-	51.01	-	-
$S0 + S3 + S4$	147.53	-	-	<u>174.49</u>	<u>2882.23</u>
$S3 + S4$	-	-	-	185.87	3488.25

Phenomenon 2. For the second issue, we train the counting models only using the data with a single category, $S1$, $S2$, and $S3 + S4$ respectively. Removing the impacts of the negative samples, the model is trained on the data of $S1 + S2 + S3 + S4$. The concrete performance is illustrated in Table 5. According to the results, training each class individually is far better than training together. To be specific, MAE decreases by **36.6%**, **25.7%**, **22.2%** and **12.7%** on the four classes, respectively. The main reason is that NWPU-Crowd contains more diverse crowd scenes than the previous datasets. There are large appearance variations in the dataset, especially the scales of the head. At present, the existing models can not tackle this problem well.

4.6 The Effectiveness of Negative Samples

In Section 3.3, we mention that the Negative Samples (“NS” for short) can effectively improve the generalization ability of the model. Here, we conduct four groups of comparative experiments using C3F-VGG [38] to verify this opinion. To be specific, there are four types of training data: $S1$, $S2$, $S3 + S4$ and $S1 + \dots + S4$. We respectively train the models for them using NS and without NS. In other words, we add $S0$ to the above four types of training data. The concrete results are reported in Table 5. After introducing NS, the category-wise MAEs are significantly remedied. Take the last six rows as the examples, the MAE is respectively decreased by **21.7%**, **2.0%**, **6.1%** and **17.4%** on the category-wise evaluation. The main reason is that NS contains diverse background objects with different structured information, which can prompt the counting models to learn more discriminative features than ever before.

5 CONCLUSION AND OUTLOOK

In this paper, a large-scale NWPU-Crowd counting dataset is constructed, which has the characteristics of high resolution, negative samples, and large appearance variation. At the same time, we develop an online benchmark website to fairly evaluate the performance of counting models. Based on the proposed dataset, we perform the nine typical algorithms and rank them from the perspective of the counting performance, the density map quality, and the time complexity.

According to the quantitative and qualitative results, we find some interesting phenomena and some new problems that need to be addressed on the proposed dataset:

- 1) **How to improve the anti-noise capacity of the models?** In the real world, the counting model may encounter many unseen data, giving incorrect estimation for background regions. Thus, the performance on negative samples is vital in the crowd counting, which represents the models’ anti-noise capacity.
- 2) **How to remedy the inter-category impacts?** Due to the large appearance variations, the training with all data results in an obvious performance reduction compared with the individual training for each category. Hence, it is essential to prompt the counting model’s capacity for appearance representations.
- 3) **How to reduce the estimation errors in the extremely congested crowd scenes?** Because of head occlusions, small objects, and lack of structured information, the existing models can not work well in the high-density regions. From the results of the leaderboard, the current models perform poorly on $S4$.

In the future, we will continue to focus on handling the above issues and dedicate to improving the performance of crowd counting in the real world.

REFERENCES

- [1] V. A. Sindagi and V. M. Patel, “Generating high-quality crowd density maps using contextual pyramid cnns,” in *Proceedings of the IEEE International Conference on Computer Vision*, 2017, pp. 1879–1888.
- [2] X. Liu, J. Van De Weijer, and A. D. Bagdanov, “Exploiting unlabeled data in cnns by self-supervised learning to rank,” *IEEE transactions on pattern analysis and machine intelligence*, 2019.

- [3] J. Wan, W. Luo, B. Wu, A. B. Chan, and W. Liu, "Residual regression with semantic prior for crowd counting," in *Proceedings of the IEEE Conference on Computer Vision and Pattern Recognition*, 2019, pp. 4036–4045.
- [4] L. Zhang, Z. Shi, M.-M. Cheng, Y. Liu, J.-W. Bian, J. T. Zhou, G. Zheng, and Z. Zeng, "Nonlinear regression via deep negative correlation learning," *IEEE Transactions on Pattern Analysis and Machine Intelligence*, 2019.
- [5] J. Wan and A. Chan, "Adaptive density map generation for crowd counting," in *Proceedings of the IEEE International Conference on Computer Vision*, 2019, pp. 1130–1139.
- [6] A. B. Chan, Z.-S. J. Liang, and N. Vasconcelos, "Privacy preserving crowd monitoring: Counting people without people models or tracking," in *Proceedings of the IEEE conference on Computer Vision and Pattern Recognition*, 2008, pp. 1–7.
- [7] Y. Zhang, D. Zhou, S. Chen, S. Gao, and Y. Ma, "Single-image crowd counting via multi-column convolutional neural network," in *Proceedings of the IEEE conference on Computer Vision and Pattern Recognition*, 2016, pp. 589–597.
- [8] C. Zhang, K. Kang, H. Li, X. Wang, R. Xie, and X. Yang, "Data-driven crowd understanding: a baseline for a large-scale crowd dataset," *IEEE Transactions on Multimedia*, vol. 18, no. 6, pp. 1048–1061, 2016.
- [9] H. Idrees, M. Tayyab, K. Athrey, D. Zhang, S. Al-Maadeed, N. Rajpoot, and M. Shah, "Composition loss for counting, density map estimation and localization in dense crowds," *arXiv preprint arXiv:1808.01050*, 2018.
- [10] D. B. Sam, S. Surya, and R. V. Babu, "Switching convolutional neural network for crowd counting," in *Proceedings of the IEEE Conference on Computer Vision and Pattern Recognition*, vol. 1, no. 3, 2017, p. 6.
- [11] Z. Shen, Y. Xu, B. Ni, M. Wang, J. Hu, and X. Yang, "Crowd counting via adversarial cross-scale consistency pursuit," in *Proceedings of the IEEE Conference on Computer Vision and Pattern Recognition*, 2018, pp. 5245–5254.
- [12] Y. Li, X. Zhang, and D. Chen, "Csrnet: Dilated convolutional neural networks for understanding the highly congested scenes," in *Proceedings of the IEEE Conference on Computer Vision and Pattern Recognition*, 2018, pp. 1091–1100.
- [13] V. Ranjan, H. Le, and M. Hoai, "Iterative crowd counting," *arXiv preprint arXiv:1807.09959*, 2018.
- [14] L. Liu, Z. Qiu, G. Li, S. Liu, W. Ouyang, and L. Lin, "Crowd counting with deep structured scale integration network," in *Proceedings of the IEEE International Conference on Computer Vision*, 2019, pp. 1774–1783.
- [15] M. Everingham, L. Van Gool, C. K. Williams, J. Winn, and A. Zisserman, "The pascal visual object classes (voc) challenge," *International journal of computer vision*, vol. 88, no. 2, pp. 303–338, 2010.
- [16] T.-Y. Lin, M. Maire, S. Belongie, J. Hays, P. Perona, D. Ramanan, P. Dollár, and C. L. Zitnick, "Microsoft coco: Common objects in context," in *European conference on computer vision*. Springer, 2014, pp. 740–755.
- [17] G. Neuhold, T. Ollmann, S. Rota Buló, and P. Kotschieder, "The mapillary vistas dataset for semantic understanding of street scenes," in *Proceedings of the IEEE International Conference on Computer Vision*, 2017, pp. 4990–4999.
- [18] P. Wang, X. Huang, X. Cheng, D. Zhou, Q. Geng, and R. Yang, "The apollo2 open dataset for autonomous driving and its application," *IEEE transactions on pattern analysis and machine intelligence*, 2019.
- [19] A. Geiger, P. Lenz, C. Stiller, and R. Urtasun, "Vision meets robotics: The kitti dataset," *The International Journal of Robotics Research*, vol. 32, no. 11, pp. 1231–1237, 2013.
- [20] M. Cordts, M. Omran, S. Ramos, T. Rehfeld, M. Enzweiler, R. Benenson, U. Franke, S. Roth, and B. Schiele, "The cityscapes dataset for semantic urban scene understanding," in *Proceedings of the IEEE conference on computer vision and pattern recognition*, 2016, pp. 3213–3223.
- [21] K. Chen, C. C. Loy, S. Gong, and T. Xiang, "Feature mining for localised crowd counting," in *Proceedings of the British Machine Vision Conference*, vol. 1, no. 2, 2012, p. 3.
- [22] Z. Yan, Y. Yuan, W. Zuo, X. Tan, Y. Wang, S. Wen, and E. Ding, "Perspective-guided convolution networks for crowd counting," in *Proceedings of the IEEE International Conference on Computer Vision*, 2019, pp. 952–961.
- [23] H. Idrees, I. Saleemi, C. Seibert, and M. Shah, "Multi-source multi-scale counting in extremely dense crowd images," in *Proceedings of the IEEE conference on Computer Vision and Pattern Recognition*, 2013, pp. 2547–2554.
- [24] V. A. Sindagi, R. Yasarla, and V. M. Patel, "Pushing the frontiers of unconstrained crowd counting: New dataset and benchmark method," in *Proceedings of the IEEE International Conference on Computer Vision*, 2019, pp. 1221–1231.
- [25] Q. Zhang and A. B. Chan, "Wide-area crowd counting via ground-plane density maps and multi-view fusion cnns," in *Proceedings of the IEEE Conference on Computer Vision and Pattern Recognition*, 2019, pp. 8297–8306.
- [26] Q. Wang, J. Gao, W. Lin, and Y. Yuan, "Learning from synthetic data for crowd counting in the wild," in *Proceedings of IEEE Conference on Computer Vision and Pattern Recognition (CVPR)*, 2019, pp. 8198–8207.
- [27] L. Zhang, M. Shi, and Q. Chen, "Crowd counting via scale-adaptive convolutional neural network," in *2018 IEEE Winter Conference on Applications of Computer Vision (WACV)*. IEEE, 2018, pp. 1113–1121.
- [28] X. Ding, Z. Lin, F. He, Y. Wang, and Y. Huang, "A deeply-recursive convolutional network for crowd counting," in *2018 IEEE International Conference on Acoustics, Speech and Signal Processing (ICASSP)*. IEEE, 2018, pp. 1942–1946.
- [29] D. Lian, J. Li, J. Zheng, W. Luo, and S. Gao, "Density map regression guided detection network for rgb-d crowd counting and localization," in *The IEEE Conference on Computer Vision and Pattern Recognition (CVPR)*, 2019, pp. 1821–1830.
- [30] Y. Fang, B. Zhan, W. Cai, S. Gao, and B. Hu, "Locality-constrained spatial transformer network for video crowd counting," in *2019 IEEE International Conference on Multimedia and Expo (ICME)*. IEEE, 2019, pp. 814–819.
- [31] W. Liu, M. Salzmann, and P. Fua, "Context-aware crowd counting," in *The IEEE Conference on Computer Vision and Pattern Recognition (CVPR)*, 2019, pp. 5099–5108.
- [32] R. Bahmanyar, E. Vig, and P. Reinartz, "Mrcnet: Crowd counting and density map estimation in aerial and ground imagery," *arXiv preprint arXiv:1909.12743*, 2019.
- [33] L. Wen, D. Du, P. Zhu, Q. Hu, Q. Wang, L. Bo, and S. Lyu, "Drone-based joint density map estimation, localization and tracking with space-time multi-scale attention network," *arXiv preprint arXiv:1912.01811*, 2019.
- [34] J. Johnson, A. Alahi, and L. Fei-Fei, "Perceptual losses for real-time style transfer and super-resolution," in *European conference on computer vision*. Springer, 2016, pp. 694–711.
- [35] K. Simonyan and A. Zisserman, "Very deep convolutional networks for large-scale image recognition," *arXiv preprint arXiv:1409.1556*, 2014.
- [36] X. Cao, Z. Wang, Y. Zhao, and F. Su, "Scale aggregation network for accurate and efficient crowd counting," in *Proceedings of the European Conference on Computer Vision*, 2018, pp. 734–750.
- [37] J. Gao, Q. Wang, and X. Li, "Pcc net: Perspective crowd counting via spatial convolutional network," *IEEE Transactions on Circuits and Systems for Video Technology*, 2019.
- [38] J. Gao, W. Lin, B. Zhao, D. Wang, C. Gao, and J. Wen, "C³ framework: An open-source pytorch code for crowd counting," *arXiv preprint arXiv:1907.02724*, 2019.
- [39] W. Liu, M. Salzmann, and P. Fua, "Context-aware crowd counting," in *Proceedings of the IEEE Conference on Computer Vision and Pattern Recognition*, 2019, pp. 5099–5108.
- [40] J. Gao, Q. Wang, and Y. Yuan, "Scar: Spatial-/channel-wise attention regression networks for crowd counting," *Neurocomputing*, vol. 363, pp. 1–8, 2019.
- [41] X. Wang, R. Girshick, A. Gupta, and K. He, "Non-local neural networks," in *Proceedings of the IEEE Conference on Computer Vision and Pattern Recognition*, 2018, pp. 7794–7803.
- [42] Z. Ma, X. Wei, X. Hong, and Y. Gong, "Bayesian loss for crowd count estimation with point supervision," in *Proceedings of the IEEE International Conference on Computer Vision*, 2019, pp. 6142–6151.
- [43] K. He, X. Zhang, S. Ren, and J. Sun, "Deep residual learning for image recognition," in *Proceedings of the IEEE conference on Computer Vision and Pattern Recognition*, 2016, pp. 770–778.
- [44] A. Paszke, S. Gross, F. Massa, A. Lerer, J. Bradbury, G. Chanan, T. Killeen, Z. Lin, N. Gimelshein, L. Antiga et al., "Pytorch: An imperative style, high-performance deep learning library," in *Advances in Neural Information Processing Systems*, 2019, pp. 8024–8035.
- [45] D. P. Kingma and J. Ba, "Adam: A method for stochastic optimization," *arXiv preprint arXiv:1412.6980*, 2014.
- [46] Z. Wang, A. C. Bovik, H. R. Sheikh, and E. P. Simoncelli, "Image quality assessment: from error visibility to structural similarity," *IEEE transactions on image processing*, vol. 13, no. 4, pp. 600–612, 2004.